

# Design and Evaluation of a Dipole Antenna TX/RX element as a Building Block for Combined MR imaging and RF Hyperthermia at 7.0 T

Celal Özerdem<sup>1</sup>, Lukas Winter<sup>1</sup>, Werner Hoffmann<sup>2</sup>, Helmar Waiczies<sup>1</sup>, Reiner Seemann<sup>2</sup>, Davide Santoro<sup>1</sup>, Alexander Müller<sup>1</sup>, Abdullah Ok<sup>1</sup>, Tomasz Lindel<sup>2</sup>, Bernd Ittermann<sup>2</sup>, and Thoralf Niendorf<sup>1,3</sup>

<sup>1</sup>Berlin Ultrahigh Field Facility (B.U.F.F.), Max-Delbrueck-Center for Molecular Medicine, Berlin, Germany, <sup>2</sup>Physikalisch Technische Bundesanstalt (PTB), Berlin, Germany, <sup>3</sup>Experimental and Clinical Research Center (ECRC), Charité - University Medicine Campus Berlin Buch, Berlin, Germany

## Introduction:

Dipole antennas can be considered as an alternative for transmit-receive coil arrays tailored for ultra-high field MRI. Dipole antenna configurations offer improvements in signal-to-noise-ratio (SNR) and  $B_{1+}$  efficiency versus loop element or strip element configurations [1-2]. The traits of radiative elements are also useful for radio frequency (RF) hyperthermia which is of proven clinical value as an adjunctive therapy for established cancer treatments like radiotherapy and chemotherapy [3-4]. Realizing these opportunities this work proposes a bow-tie dipole antenna building block and examines its capabilities for MR imaging and its properties for RF-heating at 297MHz in an attempt to explore the feasibility of an multi-channel hybrid hyperthermia-imaging coil configuration for ultra-high fields (7.0 T). To meet these goals numerical field simulations were performed to analyze the imaging and heating properties. Validation experiments were carried out in phantoms.

## Materials and Methods:

Numerical field simulations of a  $\lambda/2$  bow-tie shaped antenna were performed on a phantom with CST Microwave Studio (CST GmbH, Darmstadt, Germany). The simulated fields were evaluated in terms of  $B_{1+}$ , specific absorption rate (SAR) and temperature distribution. To shorten the wavelength of the antenna at 297 MHz distilled water with MnCl (0.7g/l) was used as a high permittivity medium. MnCl (0.7g/l) was added to shorten  $T_2^*$  and suppress the water signal for imaging. To validate the simulated data a rectangular phantom was built containing agarose gel ( $\epsilon_r=75$ ,  $\sigma=0.73$  S/m) (Fig. 1). The conductivity value was chosen based on simulated data [5]. CuSO<sub>4</sub> was added to shorten  $T_1$  for fast MR temperature measurements. A matrix of 8x8 polyethylene terephthalate (PET) tubes was integrated into the gel for temperature measurements with optical thermo sensors (LumaSense Technologies, Santa Clara, USA). For high power endurance two voltage-proof (NMNT10-12FS and NMNT18ENL, Voltronics, Salisbury, U.S.A.) nonmagnetic trimmers (max. withstanding voltage 12 kV) were used as matching and tuning capacitances. B1-mapping, MR imaging and RF heating were performed on a 7.0T whole body MR system (Magnetom, Erlangen, Germany). For B1-mapping a preparation pulse method was used. A custom built RF-Amplifier (2 channels, Max Power 2x300W (avg), frequency 100-500MHz) with a power of 100W (avg) was used for heating. MR temperature measurements were performed using the proton resonance frequency shift (PRFS) method [6]. For the heating setup the bow tie antenna and the heating phantom were placed in a birdcage coil (diameter: 27 cm, Siemens, Erlangen, Germany).

## Results:

The antenna provided images of the phantom free of artifacts. The MnCl solution didn't affect the imaging properties significantly. A closer examination revealed good agreement between the simulated and measured B1+ maps (Fig. 2). Heating of the phantom at 297 MHz was accomplished with the radiative antenna. For a heating period of 12 min using 100 Watt continuous wave a temperature increase of 5°C was observed for a region of interest placed 40 mm below the phantoms interface to the bow-tie antenna (Fig. 3). Power absorption in the permittivity medium caused a temperature increase of app 10 degrees in this medium. For deep lying regions (distance to the surface of the antennas permittivity medium larger than 15mm) the simulated temperature maps showed temperature changes due to RF heating similar to the measured temperature changes. For regions close to the surface of the bow-tie antennas interface a discrepancy between the simulated and the measured temperatures changes was observed.

## Discussion and Conclusion:

This work demonstrates that bow-tie dipole antenna configurations used here afford hybrid imaging/RF heating at ultra-high fields. The TX/RX element proposed here is well suited as a building block for a multi-channel TX/RX hybrid imaging/RF heating architecture at 7.0 T. To further improve imaging as well as heating performance we anticipate to use deuterium oxide (heavy water) as permittivity medium. This approach will reduce power losses in the permittivity medium and hence will help to reduce if not eliminate heating of the antenna. The MR temperature measurements need further refinement in order to produce artifact free and accurate temperature maps. Temperature simulation parameters need to be refined in order to produce accurate temperature maps in the surface area.

## References:

[1] Raaijmakers, A., et al., MRM, 2011; [2] Lattanzi, R. and D.K. Sodickson, ISMRM Proc, 2011; [3] Wust, P., et al., Int J of Hyperthermia, 1996; [4] Issels, R.D., et al., Lancet Oncol, 2010; [5] Yang, Q.X., et al., MRM, 2004; [6] Wonneberger, U., et al., JMRI, 2010

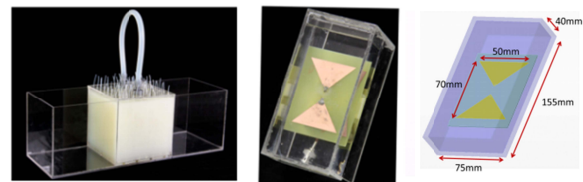


**Fig. 1:** Box phantom (left) filled with agarose gel ( $\epsilon_r=75$ ,  $\sigma=0.73$  S/m) with dimensions  $510 \times 20 \times 20$  mm<sup>3</sup>. Agarose gel contains 20g/l agarose, 3.33 g/l NaCl and 0.75g/l CuSO<sub>4</sub>. Bow tie antenna (middle) and its dimensions (right).

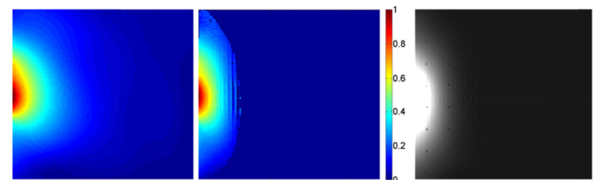


**Fig. 2:** Normalized simulated (left) and measured (middle) B1+ maps. Gradient echo image (right) of the phantom.

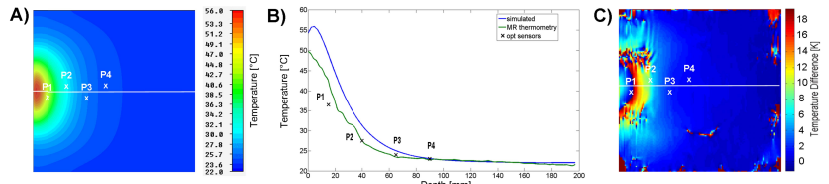


**Fig. 3:** A) Simulated temperature distribution and positions of optical thermo sensors. B) Simulated (blue line) and measured (green line) temperature along a profile with the corresponding optical thermo sensor measurements P1 (15mm distance), P2 (40mm distance), P3 (65mm distance) and P4 (90mm distance). C) Measured temperature distribution using the PRFS method.